Full Paper

# Synthesis of Some New 3-Coumaranone and Coumarin Derivatives as Dual Inhibitors of Acetyl- and Butyrylcholinesterase

**Masoumeh Alipour[1], Mehdi Khoobi[2], Hamid Nadri[3], Amirhossein Sakhteman[3], Alireza Moradi[3], Mehdi Ghandi[1], Alireza Foroumadi[2], and Abbas Shafiee[2]**

[1] School of Chemistry, University College of Science, University of Tehran, Tehran, Iran
[2] Department of Medicinal Chemistry, Faculty of Pharmacy and Pharmaceutical Sciences Research Center, Tehran University of Medical Sciences, Tehran, Iran
[3] Department of Medicinal Chemistry, Faculty of Pharmacy, Shahid Sadoughi University of Medical Sciences, Yazd, Iran

A novel series of coumarin and 3-coumaranone derivatives encompassing the phenacyl pyridinium moiety were synthesized and evaluated for their acetylcholinesterase (AChE) and butyrylcholinesterase (BuChE) inhibitory activity using Ellman's method. All compounds presented inhibitory activity against both AChE and BuChE in the micromolar range. The molecular docking simulations revealed that all compounds were dual binding site inhibitors of AChE. A kinetic study was performed and the mechanism of enzyme inhibition was proved to be of mixed type. All compounds were tested for their antioxidant activity and no significant activity was observed.

**Keywords:** Actylcholinesterase / Butyrylcholinesterase / Coumarin / 3-Coumaranone / Docking study / Phenacyl pyridinium

Received: March 8, 2013; Revised: April 10, 2013; Accepted: April 12, 2013

DOI 10.1002/ardp.201300080

## Introduction

Acetylcholinesterase, is a key enzyme in the central nervous system that is responsible for hydrolyzing acetylcholine (Ach) particularly in cortex and hippocampus [1]. According to the cholinergic hypothesis inhibition of AChE in the two aforementioned parts of the brain can alleviate the sign and symptoms of Alzheimer's disease (AD) [2]. Donepezil, rivastigmaine, galanthamine, and tacrine are the most known and clinically applied AChE inhibitors that have been approved by the United States Food and Drug Administration (FDA) for treating AD [3]. There are two distinct ligand binding sites in the narrow gorge of AChE that are located in the gorge rim and at the bottom of the gorge named peripheral anionic site (PAS) and acylation site (ACS), respectively [1, 4, 5]. It was revealed that the dual binding site inhibitors such as donepezil exert better pharmacological profile rather than propidium, a PAS binder inhibitor, or tacrin, an ACS binder inhibitor [6, 7]. Therefore, designing dual binder inhibitors can open a new way to combat AD. Based on these findings, some bivalent ligands were synthesized using hybrid formation strategy such as tacrine-melatonin hybrids [8] and tacrine-heteroaromatic group [9].

Butyrylcholinesterase (BuChE) is another important enzyme that co-localized with AChE in the brain with the lower capacity for hydrolyzing of Ach [10, 11]. Recent studies showed that the inhibition of BuChE along with AChE may take an important role to improve AD's symptoms. In fact maintenance of the AChE/BuChE activity ratio in AD may be vital to better management of the disease [12, 13]. Following this rationale, several dual AChE-BuChE inhibitors were synthesized and evaluated [14–16].

Coumarins (2-chromenone) as naturally occurring and chemically synthesized compounds have attracted intense

**Correspondence:** Dr. Abbas Shafiee, Department of Medicinal Chemistry, Faculty of Pharmacy and Pharmaceutical Sciences Research Center, Tehran University of Medical Sciences, Tehran 14176, Iran
**E-mail**: ashafiee@ams.ac.ir
**Fax**: +98 21 66461178

interest in recent years. Coumarin derivatives have revealed wide range of biological activities such as hepatoprotective, anti-allergic, anti-HIV-1, anti-inflammatory, antifungal, antimicrobial, antiasthmatic, anti-tumor, antiviral, anti-oxidant, antinociceptive, anti-diabetic, antidepressant effects and monoamine oxidase (MAO) inhibitory activity as well [17–20]. Moreover, 3-coumaranones (3-benzofuranone) and their analogs such as aurones are a family of heterocyclic compounds which have a broad range of bioactivity and predominantly have been used as potent anticholinesterase inhibitors [21, 22]. The planarity and aromaticity of coumarin and 3-coumaranone structure is the key feature that let them interact easily with PAS through a possible π-π stacking. In addition, presence of a positively charged group in the vicinity of PAS binding part of the molecule makes the compound more active via interaction with the anionic subsite of AChE. Moreover, if this feature combines with the aromaticity, an additional interaction with an aromatic moiety of AChE will happen [23]. In accord with these findings, several compounds with positively charged substituted nitrogen have been synthesized [24–27]. In view of the above structural characteristics of the enzyme-inhibitors interaction and to achieve dual binding site inhibitors, some *N*-substituted heteroarylidene methyl pyridinium compounds were designed and synthesized as potential dual AChE-BuChE inhibitors. The designed structures encompass three distinct parts with the ability to interact with different active sites along the narrow gorge of the enzyme (Fig. 1). The activity of the target compounds has been evaluated through *in vitro* AChE-BuChE inhibition assay using Ellman's colorimetric method.

## Results and discussion

### Chemistry

The synthesis of some coumarin and 3-coumaranone derivatives comprising the phenacyl pyridinium moiety is described in this work. The synthetic pathways for the preparation of target compounds are illustrated in Schemes 1 and 2. Initially as previously reported, reaction of 2-hydroxy-3-methoxybenzaldehyde **1** and ethyl acetoacetate **2** in the presence of catalytic amount of piperidine yielded 8-methoxy-3-acethyl coumarin **3** [28]. Compound **5** was prepared via an aldol condensation of compound **3** and commercially available pyridine-4-carbaldehyde **4**. Different basic and acidic media (*p*-toluenesulfonic acid (*p*-TsOH) in toluene, KOH or gaseous HCl in ethanol, piperidine in ethanol or *n*-butanol) were employed for preparing the latter compound, using both thermal and microwave conditions. Under these conditions, a mixture of geometric isomers with the excess amount of *E*-isomer was formed, while under optimized condition including piperidine in *n*-butanol and microwave irradiation, only *E*-configuration was obtained (Scheme 1).

According to the coupling constant of 15–16 Hz between the two olefinic protons, the *E*-configuration was assigned to the exocyclic double bond. Finally, the target compounds **7a–e** were obtained via the reaction of intermediate **5** with various phenacyl halides in dry acetonitrile (Scheme 1). Compound **10** was easily prepared through the reaction of resorcinol **7** with chloroacetyl chloride **8** using $AlCl_3$ as Lewis acid followed by intramolecular cyclization with NaOH [21]. The alkylation of hydroxyl group of compound **10** using ethyl iodide in dry *N*,*N*-dimethylformamide (DMF) gave compound

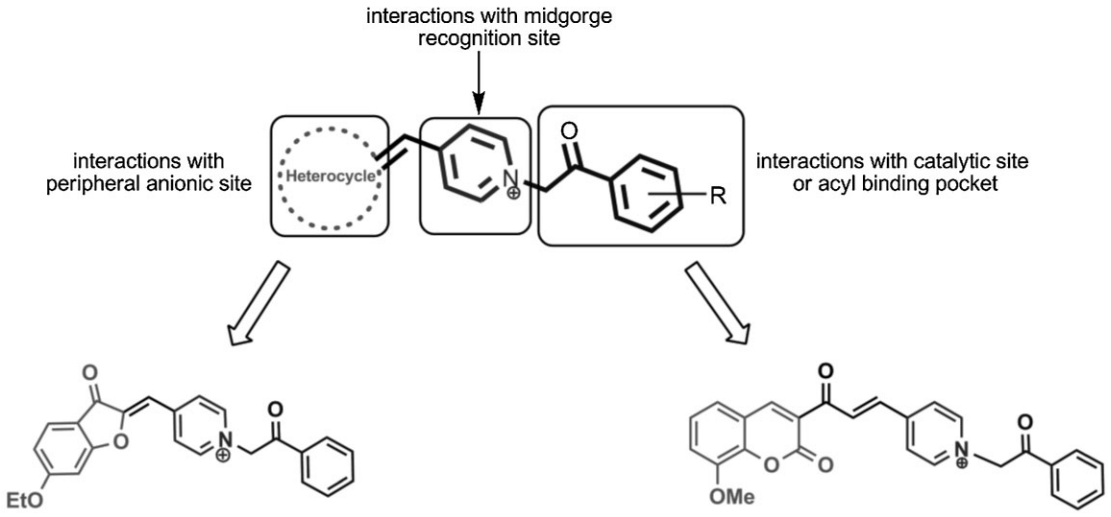


**Figure 1.** Designed structures as potential inhibitors of AChE and BuChE.

 

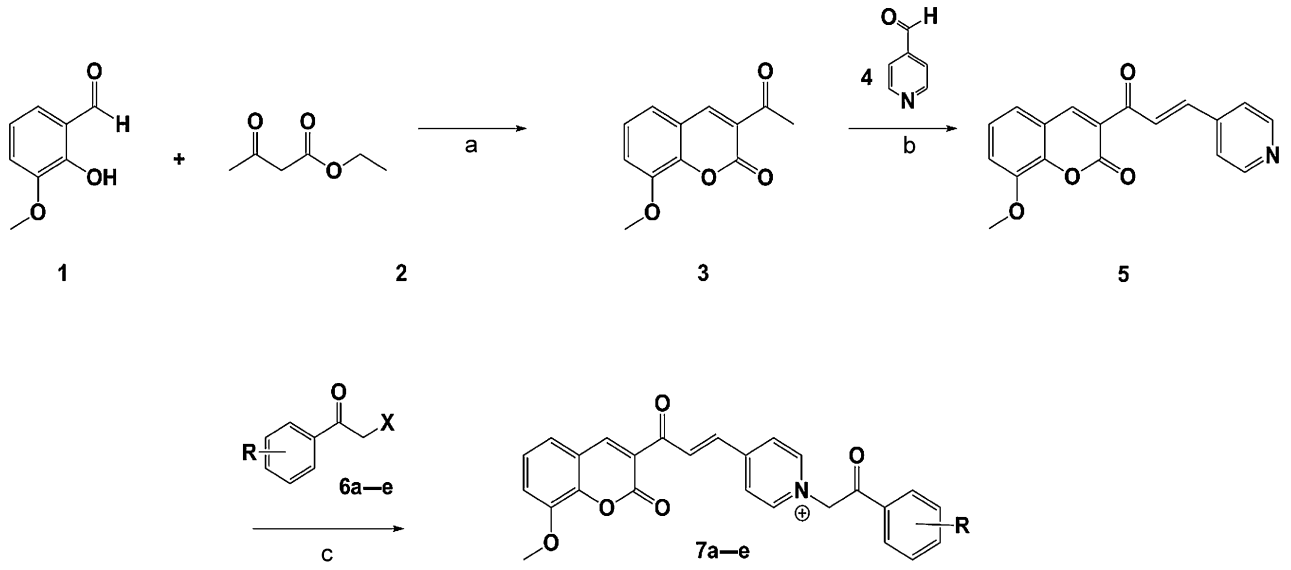


**Scheme 1.** Reagents and conditions: (a) piperidine, 50°C, 1 h; (b) piperidine, MW, 30 min; (c) phenacyl halide derivatives, dry acetonitrile, r.t., 2–3 days.

**11**. The subsequent condensation of intermediate **11** with pyridine-4-carbaldehyde **4** afforded the conjugate compound **12**.

In the case of the compound **12**, the best result was attained in the presence of *p*-TsOH in dry toluene. The $^{13}C$ NMR chemical shift of the exocyclic olefinic carbon was around 113 ppm which was attributed to the *Z*-configuration [21, 29]. Finally, compounds **12** reacted with different phenacyl halides **6** in dry acetonitrile to produce the target compounds **13a–e** (Scheme 1).

## Molecular modeling and ADME prediction

To get better insight to the interaction of tested compounds and to develop preliminary structure activity relationship (SAR), docking studies were performed using Autodock vina 1.1.1. Analysis of docking results revealed that all target compounds exhibited dual binding mode but with slightly different interactions with the receptor. The compounds are oriented towards the gorge of the enzyme in two different ways. The coumarin derivatives **7** are more prone to the catalytic site while 3-coumaranone derivatives **13** are at the

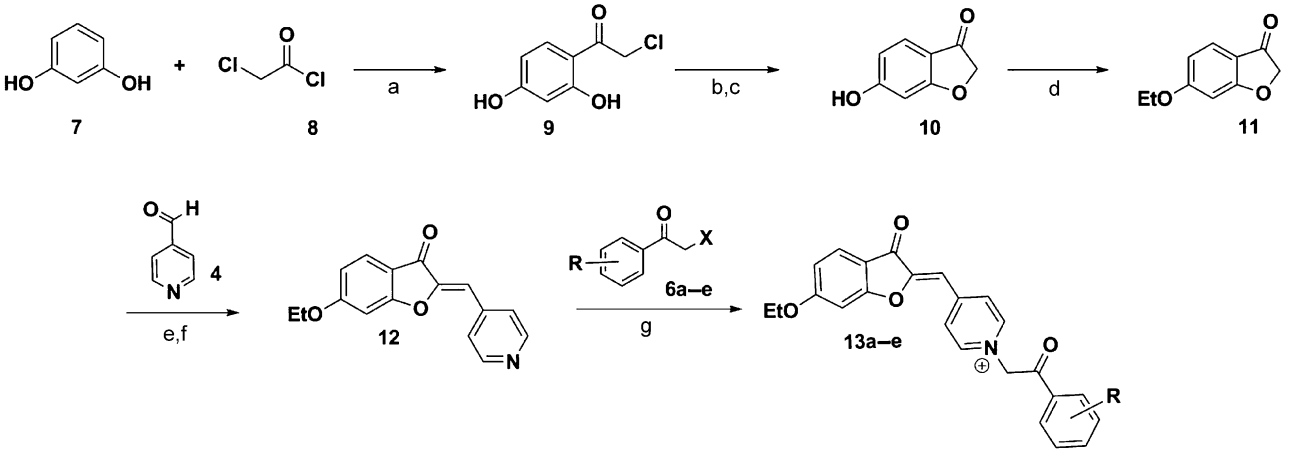


**Scheme 2.** Reagents and conditions: (a) $AlCl_3$, reflux, overnight; (b) NaOH 5%, 0°C to rt; (c) HCl 6 M; (d) ethyl iodide, anhydrous $K_2CO_3$, dry DMF, 80°C, 2 h; (e) PTSA, reflux, 3 h; (f) 10% sodium hydrogen carbonate, 30–60 min; (g) phenacyl halide derivatives, dry acetonitrile, r.t., 3–4 days.

 

vicinity of the PAS. The 3-coumaranone series **13** are well superimposed at the midgorge recognition site of the enzyme due to presence of a quaternary nitrogen in all compounds, which gives them the ability to interact with Tyr330 through formation of a π-cation bond. As illustrated in Fig. 2, all 3-coumaranone derivatives **13** were superimposed in the gorge of the enzyme except **13d**. This can be explained by the more polar property of the 3,4-dihydroxy phenacyl moiety which makes it possible to interact with the more hydrophilic region at the vicinity of the catalytic site. The complex was stabilized via two hydrogen bond interactions with Glu199. It is feasible for the longer molecule in coumarin derivatives **7** to stretch out beyond the gorge and interact with Trp84 at the proximity of the catalytic site via a π-π interaction (as depicted in Fig. 3).

Using PreADMET web-based application (http://preadmet.bmdrc.org), different pharmacokinetic properties were predicted for all target compounds such as blood-brain barrier (BBB) penetration activity, log D, percentage of human intestinal absorption (HIA) and van der Waals surface area of polar nitrogen and oxygen atoms (PSA and tPSA). The predicted data are summarized in Table 1.

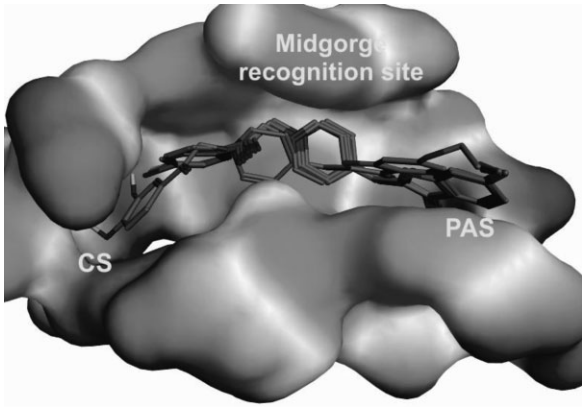


**Figure 2.** Superimpositions of the best-docked poses of compounds **13a–e** in the active site of AChE.

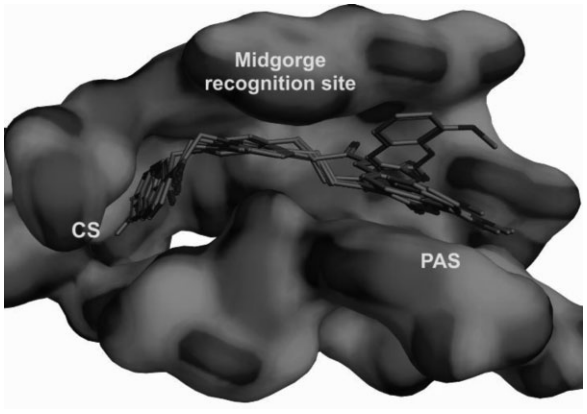


**Figure 3.** Superimpositions of the best-docked poses of compounds **7a–e** in the AChE binding site.

According to the table, all the target compounds exhibited desirable ADME properties. All of them except for **13a**, **13d**, **13e**, and **13f** may be able to penetrate into the central nervous system (CNS) and show CNS activity due to comprising suitable ADME properties such as PSA $< 60$–$70$ Å$^2$ [30].

## Biological activity

Ellman's method was used to determine anticholinesterase activity of new series of coumarin **7a–e** and 3-coumaranone **13a–e** derivatives. The activities of two series of compounds against both acetylcholinesterase and butyrylcholinesterase are summarized in Table 2. In order to investigate whether the $IC_{50}$ values are statistically different, one-way ANOVA followed by Newman–Keuls post-test was performed and the $p$-values $<0.05$ were considered as significant. Donepezil hydrochloride was used as the reference drug for both target enzymes.

Most of the compounds were active against acetylcholinesterase in the range of 1.3 to 36 μM. It was observed that 3-coumaranone derivatives were normally more potent agents than coumarin analogs against acetylcholinesterase. On the contrary, the compounds with no substituent at phenacyl substructure showed similar activities as in compounds **7c** and **13c** with $IC_{50}$ values of 10 and 7.4 μM, respectively ($p > 0.05$). This finding shows the role of substitution at phenacyl part of the compounds. Based on the $IC_{50}$ values of coumarin derivatives against AChE, the order of activity for substituents at phenacyl substructure was 4-F ≈ 4-H > 4-$CH_3$ > 4-$OCH_3$ > 4-Br. In this series the order of activity was affected by both the electron withdrawing nature and the lipophilicity of the substituents. Electron withdrawing group with low lipophilic property is well tolerated at para position as seen in compound **7d**. In contrast substituents with more electron donating property such as methyl and methoxy decreased the activity via weakening the critical π-π interaction with Trp84. Since the phenacyl group was oriented towards a hydrophilic pocket composed of Gly441, Glu199, His440, and Tyr130, the more lipophilic substituents at para position were not well accommodated in such a lipophilic pocket as in compound **7e** having bromo substituent (Fig. 4).

In addition, coumarin derivatives **7** exhibited lower activity against butyrylcholinesterase except in case of **7a** with methyl at phenacyl moiety as the most active compound in this series ($IC_{50} = 8\mu M$).

On the other hand, in 3-coumaranone series **13**, all substituents at para position of phenacyl led to an increase in the activity of the target compounds compared to **13c** with no substituent. Based on docking studies insertion of an

 

**Table 1.** *In silico* predicted ADME properties and molecular descriptors of the target compounds.

| Compounds | R | Surface area (Å$^2$) | | LogD[c] | BBB penetration | | HIA %[e] |
|---|---|---|---|---|---|---|---|
| | | PSA[a] | tPSA[b] | | C. brain/C. blood[d] | CNS absorption [38] | |
| **7a** | 4-$CH_3$ | 32.14 | 60.39 | 1.3 | 0.64 | Middle | 97.46 |
| **7b** | 4-$OCH_3$ | 34.64 | 69.62 | 0.77 | 0.37 | Middle | 97.48 |
| **7c** | H | 32.14 | 60.39 | 0.82 | 0.48 | Middle | 97.42 |
| **7d** | 4-F | 32.14 | 60.39 | 0.95 | 0.57 | Middle | 97.43 |
| **7e** | 4-Br | 32.14 | 60.39 | 1.6 | 0.73 | Middle | 98.41 |
| **13a** | 4-$CH_3$ | 45.7 | 73.55 | 1.14 | 0.097 | Low | 97.56 |
| **13b** | 4-F | 45.7 | 73.55 | 0.79 | 0.1 | Middle | 97.61 |
| **13c** | H | 45.7 | 73.55 | 0.65 | 0.11 | Middle | 97.61 |
| **13d** | 2,4-Cl | 45.7 | 73.55 | 2.02 | 0.085 | Low | 97.81 |
| **13e** | 3,4-OH | 81.89 | 114.01 | 0.33 | 0.015 | Low | 95.55 |
| **13f** | 4-Br | 45.7 | 73.55 | 1.44 | 0.082 | Low | 97.64 |
| Donepezil | – | 18.57 | 39.97 | 2.6 | 0.19 | Middle | 97.95 |

[a] Polar surface area.
[b] Topological polar surface area.
[c] Calculated in pH 7.4.
[d] The ratio of the compound concentration in brain and blood.
[e] The percent of human intestinal absorption.

electron withdrawing group enhanced the π–π stacking interactions between phenacyl and Phe330 as in case of **13b** ($p < 0.001$) and **13e** ($p < 0.01$). The enhanced activity of compound **13a** compared to **13c** ($p < 0.001$) with no substituent could be attributed to a lipophilic CH–π interaction between methyl and Trp84 (Fig. 5).

In compound **13d** with two hydroxyl groups at *meta* and *para* positions of phenacyl moiety a hydrogen bonding network with the residues at the bottom of the binding site might be responsible for the improved activity (Fig. 6).

The most active compound was compound **13b** with fluoro at *para* position of phenacyl moiety ($IC_{50} = 1.3$ μM). All compounds showed to be less selective inhibitors than the reference drug donepzil hydrochloride. Meanwhile, the compounds bearing 3-coumaranone moiety were normally more selective than those with coumarin substructure. It seems that the lower selectivity index of the target compounds makes them promising dual inhibitors of AChE/BuChE for future studies.

**Table 2.** AChE and BuChE inhibition data and their selectivity for synthesized compounds **7a–e** and **13a–e**.

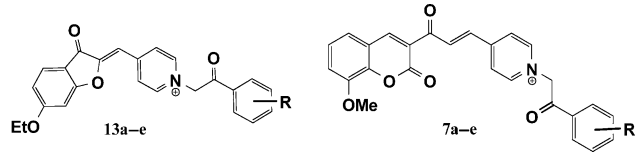


| Compound | R | $IC_{50}$ (μM)[a,b] | | Selectivity for AChE[c] |
|---|---|---|---|---|
| | | AChE | BuChE | |
| **7a** | 4-$CH_3$ | 13.5 ± 0.78 | 8.0 ± 0.22 | 0.6 |
| **7b** | 4-$OCH_3$ | 21.0 ± 1.2 | 34 ± 1.6 | 1.6 |
| **7c** | H | 10.0 ± 0.29 | 43 ± 2.3 | 4.3 |
| **7d** | 4-F | 8.2 ± 0.17 | 42 ± 3.1 | 5.1 |
| **7e** | 4-Br | 36 ± 1.9 | 51 ± 2.9 | 1.4 |
| **13a** | 4-$CH_3$ | 1.4 ± 0.12 | 28.0 ± 1.4 | 20 |
| **13b** | 4-F | 1.3 ± 0.04 | 15.8 ± 0.85 | 12.1 |
| **13c** | H | 7.4 ± 0.13 | 23.5 ± 1.1 | 3.2 |
| **13d** | 3,4-Di(OH) | 3.7 ± 0.69 | 26.7 ± 1.5 | 7.2 |
| **13e** | 4-Br | 3.0 ± 0.24 | 31 ± 1.9 | 10.3 |
| Donepezil | – | 0.014 ± 0.003 | 5.38 ± 0.17 | 384 |

[a] The concentration of inhibitor required to produce 50% enzyme inhibition.
[b] Data are means of three independent experiments ± SE.
[c] Selectivity for AChE = $IC_{50}$ (BuChE)/$IC_{50}$ (AChE).

## Kinetic study

The kinetic study was done on the most active compound, **13b**, and the compound was tested at three fixed concentrations including 1.96, 3.92, and 19.6 nM. For each concentration, the initial velocity (*V*) of the substrate hydrolysis was measured at four different substrate (*S*) concentrations in the range of 0.137–0.689 mM. Subsequently, the reciprocal of the initial velocity (1/*V*) versus the reciprocal of the substrate concentration (1/*S*) was plotted. Based on the Lineweaver–Burk plot depicted in Fig. 7, a pattern of increasing slopes and intercepts with higher inhibitor concentrations was obtained. This pattern was representing a mixed type inhibition for the compounds of this series. The result of this study was in accord with docking studies regarding the dual binding mode of the target compounds.

 

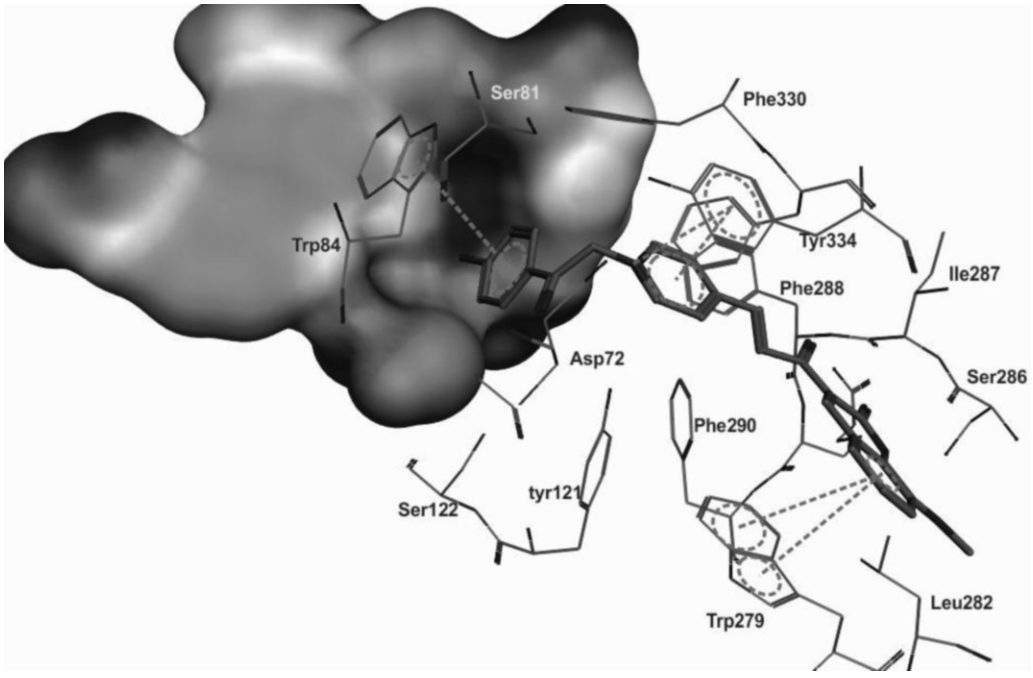


**Figure 4.** Interaction of compound **7e** docked into the binding site of AChE. The hydrophobic bromo substituent of **7e** is oriented toward a hydrophilic pocket of active site.

## Total antioxidant activity

Since oxidative stress proved to be a key feature of AD that is determined by increased oxidative markers including DNA, RNA, lipid, and protein oxidation [31, 32], using antioxidant compounds may be beneficial to treat AD symptoms. Thus, total antioxidant activity of the final compounds was measured using FRAP (ferric reducing antioxidant power) assay and FRAP values of the target compounds are presented in Table 3. As it

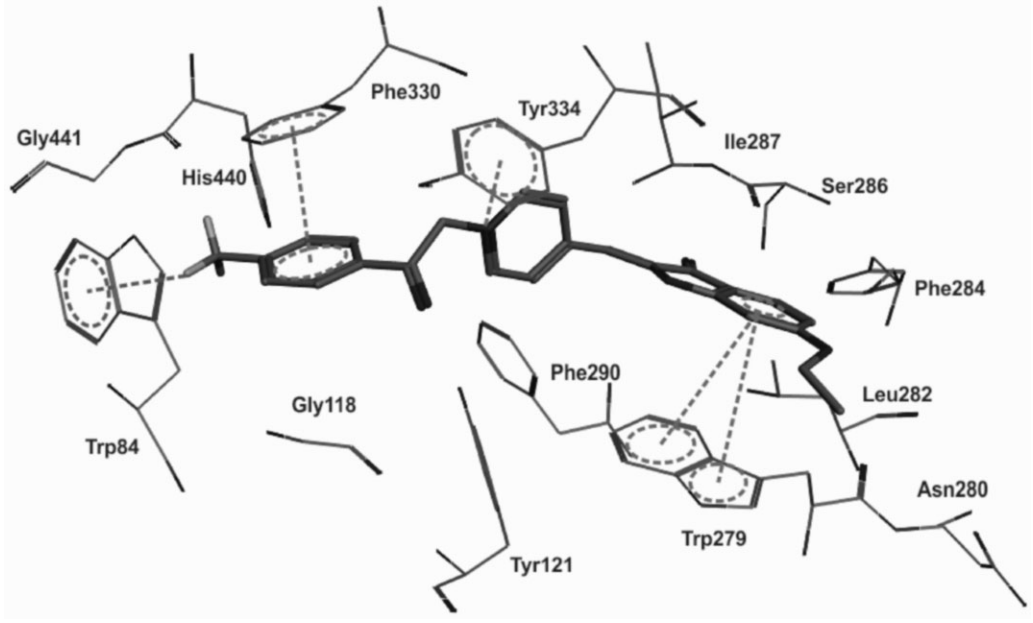


**Figure 5.** The interacting mode of compound **13a** in the active site of AChE.

 

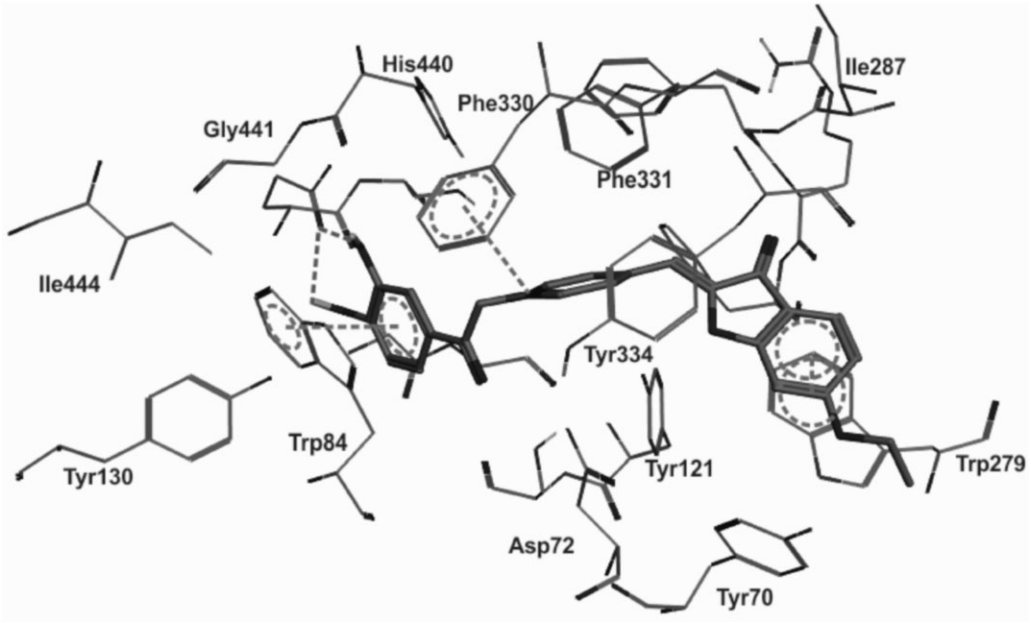


**Figure 6.** The interacting mode of compound **13d** in the active site of AChE.

can be seen in the table, none of the compounds showed significant antioxidant activity in comparison to ascorbic acid as reference drug, except for compounds **7b** and **13d**. The considerable antioxidant activity of compound **7b** and **13d** could be attributed to presence of methoxy group and catechol group on phenacyl moiety, respectively.

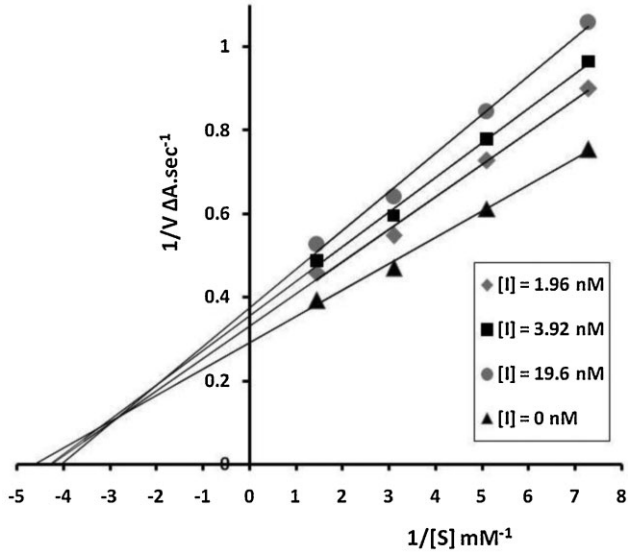


**Figure 7.** Steady-state Lineweaver–Burk plot of compound **13b**, against acetylcholinesterase enzyme. The plot is based on the reciprocal of initial velocity and reciprocal of substrate concentration at increasing inhibitor concentrations.

## Conclusion

A novel series of some coumarin and 3-coumaranone derivatives linking to phenacyl pyridinium moiety were designed as dual binding site cholinesterase inhibitors. The synthesized compounds were tested in terms of their inhibitory potency against both AChE and BuChE. The spectrophotometric method of Ellman was used for AChE/BuChE inhibitory activity. All synthesized compounds showed to be moderately potent dual inhibitors of AChE and BuChE, with $IC_{50}$ values ranging in micromolar. Compound **13b** was subjected for kinetic study and it showed the mixed type of

**Table 3.** The antioxidant activities of the compounds **7a–e** and **13a–e**.

| Compounds | FRAP-value[a)] |
|---|---|
| **7a** | NA |
| **7b** | **159** |
| **7c** | NA |
| **7d** | NA |
| **7e** | NA |
| **13a** | NA |
| **13b** | NA |
| **13c** | NA |
| **13d** | **676** |
| **13e** | NA |
| Ascorbic acid | 2975 |

NA, no activity.
[a)] FRAP value is expressed as mmol Fe(II)/g.

 

inhibition toward the AChE. These results are in agreement with the conclusions of docking studies in which all target compounds interacted with both the CAS and PAS of AChE.

## Experimental

### Chemistry

All commercially available reagents were purchased from Merck AG, Aldrich or Acros Organics and used without further purification. Column chromatography was carried out on silica gel (70–230 mesh). TLC was conducted on silica gel 250 micron, F254 plates. The 3-acetylcoumarin **3** and 6-ethoxybenzofuran-3(2*H*)-one **11** were prepared by the reported methods [21, 28]. For the synthesis of compounds **5** the experiments were performed using a microwave oven (ETHOS 1600, Milestone) with a power of 600 W, specially designed for an organic synthesis and modified with a condenser and mechanical stirrer. Melting points were measured on a Kofler hot stage apparatus and are uncorrected. The IR spectra were taken using Nicolet FT-IR Magna 550 spectrographs (KBr disks). Mass spectra of the products were obtained with an HP (Agilent Technologies) 5937 mass selective detector. $^1$H NMR spectra were recorded on a Varian 400 or Bruker 500 MHz NMR instruments. The atoms numbering of the target compounds used for $^1$H NMR data are depicted in Fig. 8. The chemical shifts ($\delta$) and coupling constants ($J$) are expressed in parts per million and Hertz, respectively. The results of elemental analyses (C, H, N) were within ±0.4% of the calculated values.

#### *Representative procedure for the preparation of 8-methoxy-3-acetyl coumarin (**3**)*

To a cold mixture of 2-hydroxy-3-methoxy benzaldehyde **1** (0.2 mol) and ethyl acetoacetate **2** (0.2 mol), a few drops of piperidine were added by rapid stirring. The mixture was allowed to warm to 50°C. When the reaction was finished (monitored by TLC), the yellow solid was filtered off and subsequently washed with ethanol and crystallized from water/ethanol (30:70) [28].

#### *Representative procedure for the preparation of (E)-8-methoxy-3-(3-(pyridin-4-yl)acryloyl)-2H-chromen-2-one (**5**)*

To a stirring mixture of 8-methoxy-3-acetyl coumarin **3** (1 mmol) and pyridine-4-carbaldehyde **4** (1.2 mmol) in 3 mL *n*-butanol were added catalytic amounts of piperidine (2 drops). The mixture was irradiated with microwaves at 150°C for 30 min. After completion of the reactions, the mixture was cooled and the solid was filtered off and washed with ethanol. The organic phase was evaporated and the residue was purified by silica gel column chromatography using petroleum ether/ethyl acetate (70:30) as the mobile phase to give the further pure product.

#### *General procedure for the synthesis of (E)-4-(3-(8-methoxy-2-oxo-2H-chromen-3-yl)-3-oxoprop-1-enyl)-1-(2-oxo-2-phenylethyl)pyridinium halides **7a–e***

To a solution of (*E*)-8-methoxy-3-(3-(pyridin-4-yl)acryloyl)-2*H*-chromen-2-one **5** (1 mmol) in dry acetonitrile (7 mL), different phenacyl halides **6** (1.2 equiv) and catalytic amount of KI were added. The reaction mixture was stirred at room temperature for 2–3 days. Progress of the reaction was monitored by TLC. After completion of the reaction, the solid was filtered off and washed with acetonitrile to give compound **7**. The solids were further purified if needed by flash chromatography using chloroform/methanol (99:1) as the mobile phase.

#### *(E)-4-(3-(8-Methoxy-2-oxo-2H-chromen-3-yl)-3-oxoprop-1-enyl)-1-(2-oxo-2-p-tolylethyl)pyridinium bromide (**7a**)*

Yield 75%, orange solid, mp 183–185°C, IR $\upsilon_{max}$/cm$^{-1}$ (KBr): 1760, 1716 and 1679 (C=O), $^1$H NMR (DMSO$d_6$, 400 MHz), 9.02 (d, 2H, $H_a$-pyridine, $J$ = 6.4 Hz), 8.82 (s, 1H, $H_4$ coumarin), 8.54 (d, 2H, $H_b$-pyridine, $J$ = 6.4 Hz), 8.15 (d, 1H, $H_\beta$ vinylic, $J$ = 16.4 Hz), 7.97 (d, 2H phenyl, $J$ = 8.4 Hz), 7.87 (d, 1H, $H_\alpha$ vinylic, $J$ = 16.4 Hz), 7.55–7.38 (m, 5H, 2H phenyl and $H_{5,6,7}$ coumarin), 6.44 (s, 2H, $-CH_2N^+$), 3.95 (s, 3H, OMe), 2.45 (s, 3H, Me). EI-MS *m*/*z* (%) 440 ($M^+$, 6), 439 (22), 320 (56), 119 (100), 91 (95). Anal. calcd. for $C_{27}H_{22}BrNO_5$: C, 62.32; H, 4.26; N, 2.69. Found: C, 62.18; H, 4.51; N, 2.38.

#### *(E)-4-(3-(8-Methoxy-2-oxo-2H-chromen-3-yl)-3-oxoprop-1-enyl)-1-(2-(4-methoxyphenyl)-2-oxoethyl)pyridinium bromide (**7b**)*

Yield 68%, yellow solid, mp 257–259°C, IR $\upsilon_{max}$/cm$^{-1}$ (KBr): 1755, 1717 and 1675 (C=O), $^1$H NMR (DMSO-$d_6$, 400 MHz), 8.99 (d, 2H, $H_a$-pyridine, $J$ = 6.4 Hz), 8.81 (s, 1H, $H_4$ coumarin), 8.54 (d, 2H, $H_b$-pyridine, $J$ = 6.4 Hz), 8.17 (d, 1H, $H_\beta$ vinylic, $J$ = 16.4 Hz), 8.05 (d, 2H phenyl, $J$ = 8.0 Hz), 7.87 (d, 1H, $H_\alpha$ vinylic, $J$ = 16.4 Hz), 7.53–7.38 (m, $H_{5,6,7}$ coumarin), 7.19 (d, 2H phenyl, $J$ = 8.0 Hz), 6.39 (s, 2H, $-CH_2N^+$), 3.96 (s, 3H, OMe), 3.90 (s, 3H, OMe). Anal. calcd. for $C_{27}H_{22}BrNO_6$: C, 60.46; H, 4.13; N, 2.61. Found: C, 60.17; H, 4.38; N, 2.39.

#### *(E)-4-(3-(8-Methoxy-2-oxo-2H-chromen-3-yl)-3-oxoprop-1-enyl)-1-(2-oxo-2-phenylethyl)pyridinium chloride (**7c**)*

Yield 60%, orange solid, mp 189–191°C, IR $\upsilon_{max}$/cm$^{-1}$ (KBr): 1757, 1715 and 1681 (C=O), $^1$H NMR (DMSO-$d_6$, 400 MHz), 9.03 (d, 2H, $H_a$-pyridine, $J$ = 6.4 Hz), 8.83 (s, 1H, $H_4$ coumarin), 8.55 (d, 2H, $H_b$-pyridine, $J$ = 6.4 Hz), 8.18 (d, 1H, $H_\beta$ vinylic, $J$ = 16.4 Hz), 8.08

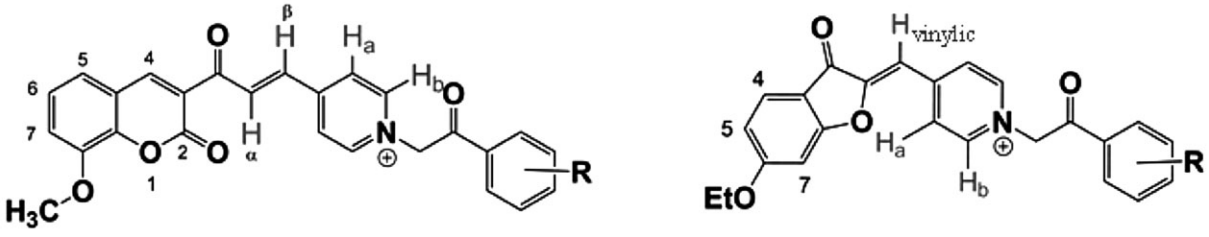


**Figure 8.** The atoms numbering of the target compounds.

 

(d, 2H phenyl, $J = 7.2$ Hz), 7.87 (d, 1H, $H_\alpha$ vinylic, $J = 16.0$ Hz), 7.80 (t, 1H phenyl, $J = 7.2$ Hz), 7.69 (d, 2H phenyl, $J = 7.2$ Hz), 7.55–7.40 (m, $H_{5,6,7}$ coumarin), 6.48 (s, 2H, $-CH_2N^+$), 3.96 (s, 3H, OMe). EI-MS *m/z* (%) 426 ($M^+$, 5), 425 (19), 320 (87), 307 (72), 105 (100), 77 (61). Anal. calcd. for $C_{26}H_{20}ClNO_5$: C, 67.61; H, 4.36; N, 3.03. Found: C, 67.33; H, 4.58; N, 2.91.

### *(E)-1-(2-(4-Fluorophenyl)-2-oxoethyl)-4-(3-(8-methoxy-2-oxo-2H-chromen-3-yl)-3-oxoprop-1-enyl)pyridinium bromide (**7d**)*

Yield 73%, brown solid, mp 190–192°C, IR $\upsilon_{max}/cm^{-1}$ (KBr): 1757, 1715 and 1681 (C=O), $^1H$ NMR (DMSO-$d_6$, 400 MHz), 8.99 (d, 2H, $H_a$-pyridine, $J = 6.4$ Hz), 8.82 (s, 1H, $H_4$ coumarin), 8.54 (d, 2H, $H_b$-pyridine, $J = 6.4$ Hz), 8.20–8.16 (m, 3H, 2H phenyl and $H_\beta$ vinylic), 7.87 (d, 1H, $H_\alpha$ vinylic, $J = 15.6$ Hz), 7.55–7.48 (m, 4H, 2H phenyl and $H_{5,7}$ coumarin), 7.40 (t, 1H, $H_6$ coumarin, $J = 8.0$ Hz), 6.43 (s, 2H, $-CH_2N^+$), 3.95 (s, 3H, OMe). EI-MS *m/z* (%) 444 ($M^+$, 5), 443 (19), 320 (74), 306 (31), 123 (100), 95 (43). Anal. calcd. for $C_{26}H_{19}BrFNO_5$: C, 59.56; H, 3.65; N, 2.67. Found: C, 59.32; H, 3.37; N, 2.90.

### *(E)-1-(2-(4-Bromophenyl)-2-oxoethyl)-4-(3-(8-methoxy-2-oxo-2H-chromen-3-yl)-3-oxoprop-1-enyl)pyridinium bromide (**7e**)*

Yield 70%, yellow solid, mp 252–254°C, IR $\upsilon_{max}/cm^{-1}$ (KBr): 1718 and 1676 (C=O), $^1H$ NMR (DMSO-$d_6$, 400 MHz), 9.00 (d, 2H, $H_a$-pyridine, $J = 6.4$ Hz), 8.82 (s, 1H, $H_4$ coumarin), 8.56 (d, 2H, $H_b$-pyridine, $J = 6.4$ Hz), 8.18 (d, 1H, $H_\beta$ vinylic, $J = 16.4$ Hz), 7.99 (d, 2H, Ph, $J = 8.0$ Hz), 7.89 (m, 3H, $H_\alpha$ vinylic and 2H phenyl), 7.55–7.40 (m, $H_{5,6,7}$ coumarin), 6.45 (s, 2H, $-CH_2N^+$), 3.95 (s, 3H, OMe). EI-MS *m/z* (%) 507 ($M^+$+2, 4), 505 ($M^+$, 6), 320 (100), 307 (50), 185 (85), 183 (87). Anal. calcd. for $C_{26}H_{19}Br_2NO_5$: C, 53.36; H, 3.27; N, 2.39. Found: C, 53.02; H, 3.51; N, 2.13.

### *Representative procedure for the preparation of 6-ethoxybenzofuran-3(2H)-one (**11**)*

To a mixture of 6-hydroxybenzofuran-3(2*H*)-one **10** (12 mmol, 1.8 g) and anhydrous potassium carbonate (1 equiv) in 5 mL dry DMF, ethyl iodide (12 mmol, 1.872 g) was added and the mixture was stirred under argon for 2 h at 80°C. Water (20 mL) was added and afterward the mixture was cooled and the mixture was extracted with ethyl acetate (3 × 30 mL). The combined organic extracts were dried over $Na_2SO_4$ and the solvent was removed under reduced pressure. The resulted oil was purified by column chromatography using petroleum ether/ethyl acetate (60:40) as the mobile phase to afford compound **11** in good yield [21].

### *6-Ethoxybenzofuran-3(2H)-one (**11**)*

Yield 86%, orange solid, mp 113–115°C, $^1H$ NMR ($CDCl_3$, 500 MHz), 7.56 (d, 1H, $H_4$ coumaranone, $J = 8.6$ Hz), 6.61 (dd, 1H, $H_5$ coumaranone, $J = 8.6$ Hz, $J = 2.2$ Hz), 6.53 (d, 1H, $H_7$ coumaranone, $J = 2.2$ Hz) 4.61 (s, 2H, CO-$CH_2$), 4.1 (q, 2H, $OCH_2$, $J = 6.8$ Hz), 1.45 (t, 3H, $-CH_3$, $J = 6.8$ Hz), EI-MS *m/z* (%) 178 ($M^+$, 100), 135 (88), 47 (79).

### *General procedure for the synthesis of (Z)-6-ethoxy-2-(pyridin-4-ylmethylene)benzofuran-3(2H)-one (**12**)*

6-Ethoxybenzofuran-3(2*H*)-one **11** (1 equiv), pyridine-4-carboxaldehyde (1.4 equiv) and PTSA (1.5 equiv) were suspended in toluene (25 mL) and heated to reflux using water separator for 3 h. The resulting mixture was cooled to 25–40°C and the solid was filtered. Further the wet solid was suspended in aqueous 10% sodium hydrogen carbonate solution (50 mL) and stirred for 30–60 min at room temperature. The resulting precipitate solid was filtered and washed with water (50 mL) and dried. The crude solid was purified by crystallization from acetonitrile [21].

### *(Z)-6-Ethoxy-2-(pyridin-4-ylmethylene)benzofuran-3(2H)-one (**12**)*

Yield 86%, orange solid, mp 113–115°C, $^1H$ NMR ($CDCl_3$, 500 MHz), 7.56 (d, 1H, $H_4$ coumaranone, $J = 8.6$ Hz), 6.61 (dd, 1H, $H_5$ coumaranone, $J = 8.6$ Hz, $J = 2.2$ Hz), 6.53 (d, 1H, $H_7$ coumaranone, $J = 2.2$ Hz), 4.1 (q, 2H, $OCH_2$, $J = 6.8$ Hz), 1.45 (t, 3H, $CH_3$, $J = 6.8$ Hz), EI-MS *m/z* (%) 178 ($M^+$, 100), 135 (88), 47 (79).

### *General procedure for the synthesis of (Z)-4-((6-ethoxy-3-oxobenzofuran-2(3H)-ylidene)methyl)-1-(2-oxo-2-phenylethyl)pyridinium halides **13a–e***

To a solution of **12** (1 mmol) in dry acetonitrile (7 mL), different phenacyl halides **6** (1.2 equiv) and catalytic amount of KI were added. The reaction mixture was stirred at room temperature for 3–4 days. Progress of the reaction was monitored by TLC. After completion of the reaction, the solid was filtered off and washed with acetonitrile to give compound **13**. The solids were further purified if needed by flash chromatography using chloroform/methanol (99:1) as the mobile phase.

### *(Z)-4-((6-Ethoxy-3-oxobenzofuran-2(3H)-ylidene)methyl)-1-(2-oxo-2-p-tolylethyl)pyridinium chloride (**13a**)*

Yield 77%, orange solid, mp 238–240°C, IR $\upsilon_{max}/cm^{-1}$ (KBr): 1699 (br, C=O), $^1H$ NMR (DMSO-$d_6$, 400 MHz), 9.05 (d, 2H, $H_a$-pyridine, $J = 6.4$ Hz), 8.61 (d, 2H, $H_b$-pyridine, $J = 6.4$ Hz), 7.99 (d, 2H phenyl, $J = 8.4$ Hz), 7.78 (d, H, $H_4$ coumaranone, $J = 7.8$ Hz), 7.49 (d, 2H phenyl, $J = 8.4$ Hz), 7.25 (s, 1H, $H_7$ coumaranone), 7.09 (s, 1H, H vinylic), 6.93 (d, 1H, $H_5$ coumaranone, $J = 7.8$ Hz), 6.51 (s, 2H, $-CH_2N^+$), 4.26 (q, 2H, $OCH_2$, $J = 6.4$ Hz), 2.46 (s, 3H, $CH_3$) 1.40 (t, 3H, $CH_3$, $J = 6.4$ Hz). EI-MS *m/z* (%) 400 ($M^+$, 1), 399 (13), 267 (65), 238 (88), 119 (100), 91 (48). Anal. calcd. for $C_{25}H_{22}ClNO_4$: C, 68.88; H, 5.09; N, 3.21. Found: C, 68.72; H, 5.28; N, 3.11.

### *(Z)-4-((6-Ethoxy-3-oxobenzofuran-2(3H)-ylidene)methyl)-1-(2-(4-fluorophenyl)-2-oxoethyl)pyridinium bromide (**13b**)*

Yield 74%, orange solid, mp 230–232°C, IR $\upsilon_{max}/cm^{-1}$ (KBr): 1738 (br, C=O), $^1H$ NMR (DMSO-$d_6$, 400 MHz), 9.06 (d, 2H, $H_a$-pyridine, $J = 6.4$ Hz), 8.61 (d, 2H, $H_b$-pyridine, $J = 6.4$ Hz), 8.20–8.17 (m, 2H phenyl), 7.78 (d, 1H, $H_4$ coumaranone, $J = 8.4$ Hz), 7.54–7.48 (m, 2H phenyl), 7.22 (s, 1H, $H_7$ coumaranone), 7.10 (s, 1H, H vinylic), 6.93 (d, 1H, $H_5$ coumaranone, $J = 8.4$ Hz), 6.54 (s, 2H, $-CH_2N^+$), 4.23 (q, 2H, $OCH_2$, $J = 6.5$ Hz), 1.40 (t, 3H, $CH_3$, $J = 6.5$ Hz). EI-MS *m/z* (%) 404 ($M^+$, 1), 403 (31), 385 (35), 266 (35), 239 (88), 123 (100). Anal. calcd. for $C_{24}H_{19}BrNO_4$: C, 59.52; H, 3.95; N, 2.89. Found: C, 59.31; H, 3.64; N, 2.57.

### *(Z)-4-((6-Ethoxy-3-oxobenzofuran-2(3H)-ylidene)methyl)-1-(2-oxo-2-phenylethyl)pyridinium chloride (**13c**)*

Yield 65%, orange solid, mp 214–216°C, IR $\upsilon_{max}/cm^{-1}$ (KBr): 1726 (br, C=O), $^1H$ NMR (DMSO-$d_6$, 400 MHz), 9.02 (d, 2H, $H_a$-pyridine, $J = 6.4$ Hz), 8.61 (d, 2H, $H_b$-pyridine, $J = 6.4$ Hz), 8.09 (d, 1H, $H_4$

 

coumaranone, $J = 7.8$ Hz), 7.80–7.65 (m, 5H phenyl), 7.21 (s, 1H, $H_7$ coumaranone), 7.08 (s, 1H, H vinylic), 6.91 (d, 1H, $H_5$ coumaranone, $J = 7.8$ Hz), 6.51 (s, 2H, $-CH_2N^+$), 4.25 (q, 2H, $OCH_2$, $J = 6.4$ Hz), 1.40 (t, 3H, $CH_3$, $J = 6.4$ Hz). $^{13}$C NMR (DMSO-$d_6$, 125 MHz), 190.6, 181.3, 168.6, 167.5, 152.6, 148.8, 146.1, 134.7, 133.4, 129.1, 128.2, 127.4, 126.3, 113.7, 112.7, 103.6, 98.0, 65.8, 64.9, 14.2. EI-MS *m/z* (%) 386 ($M^+$, 17), 385 (50), 267 (53), 238 (76), 221 (56), 105 (100). Anal. calcd. for $C_{24}H_{20}ClNO_4$: C, 68.33; H, 4.78; N, 3.32. Found: C, 68.18; H, 4.53; N, 3.55.

### *(Z)-1-(2-(3,4-Dihydroxyphenyl)-2-oxoethyl)-4-((6-ethoxy-3-oxobenzofuran-2(3H)-ylidene)methyl)pyridinium chloride (**13d**)*

Yield 80%, orange solid, mp 215–217°C, IR $\upsilon_{max}/cm^{-1}$ (KBr): 3300 (OH), 1704 (br, C=O), $^1$H NMR (DMSO-$d_6$, 400 MHz), 10.42 (s, 1H, OH), 9.71 (s, 1H, OH), 9.01 (d, 2H, $H_a$-pyridine, $J = 6.8$ Hz), 8.57 (d, 2H, $H_b$-pyridine, $J = 6.8$ Hz), 7.78 (d, 1H, $H_4$ coumaranone, $J = 8.0$ Hz), 7.49–7.46 (m, 2H phenyl), 7.22 (s, 1H, H vinylic), 7.08 (s, 1H, $H_7$ coumaranone), 7.00 (d, 1H phenyl, $J = 7.6$ Hz), 6.93 (d, 1H, $H_5$ coumaranone, $J = 8.0$ Hz), 6.38 (s, 2H, $-CH_2N^+$), 4.25 (q, 2H, $OCH_2$, $J = 6.8$ Hz), 1.40 (t, 3H, $CH_3$, $J = 6.8$ Hz). $^{13}$C NMR (DMSO-$d_6$, 125 MHz), 188.6, 181.4, 168.7, 167.6, 152.7, 152.3, 148.7, 146.2, 145.7, 127.3, 126.4, 125.1, 121.8, 115.6, 114.9, 113.8, 112.8, 103.7, 98.1, 65.4, 64.9, 14.3. EI-MS *m/z* (%) 418 ($M^+$, 7), 417 (2), 267 (74), 238 (79), 137 (100). Anal. calcd. for $C_{24}H_{20}ClNO_6$: C, 63.51; H, 4.44; N, 3.09. Found: C, 63.30; H, 4.71; N, 3.22.

### *(Z)-1-(2-(4-Bromophenyl)-2-oxoethyl)-4-((6-ethoxy-3-oxobenzofuran-2(3H)-ylidene)methyl)pyridinium bromide (**13e**)*

Yield 75%, orange solid, mp 236–238°C, IR $\upsilon_{max}/cm^{-1}$ (KBr): 1701 (br, C=O), $^1$H NMR (DMSO-$d_6$, 400 MHz), 9.01 (d, 2H, $H_a$-pyridine, $J = 6.0$ Hz), 8.61 (d, 2H, $H_b$-pyridine, $J = 6.0$ Hz), 8.02 (d, 2H phenyl, $J = 7.8$ Hz), 7.91 (d, 2H phenyl, $J = 7.8$ Hz), 7. 78 (d, 1H, $H_4$ coumaranone, $J = 8.0$ Hz), 7.23 (s, 1H, $H_7$ coumaranone), 7.09 (s, 1H, H vinylic), 6.93 (d, 1H, $H_5$ coumaranone, $J = 8.0$ Hz), 6.49 (s, 2H, $-CH_2N^+$), 4.25 (q, 2H, $OCH_2$, $J = 7.2$ Hz), 1.40 (t, 3H, $CH_3$, $J = 7.2$ Hz). EI-MS *m/z* (%) 467 ($M^+$+2, 3), 465 ($M^+$, 3), 267 (75), 238 (100), 185 (64), 183 (66). Anal. calcd. for $C_{24}H_{19}Br_2NO_4$: C, 52.87; H, 3.51; N, 2.57. Found: C, 52.55; H, 3.75; N, 2.38.

### *In silico* docking simulation study

For molecular modeling studies, the docking of target compounds in the active site of AChE was investigated. The pdb structure of target enzyme (PDB Code: 1EVE) was retrieved from Protein Data Bank (http://www.rcsb.org/pdb/home/home.do) as a complex with inhibitor, E2020. Then the water molecules and the native ligand were removed from the protein structure and converted to proper pdbqt format with Autodock Tools (ver. 1.5.4) [33]. The 2D structure of ligands were sketched in MarvineSketch 5.8.3, 2012, ChemAxon (http://www.chemaxon.com), and then energetically minimized and converted to 3D pdbqt format using Openbabel version (2.3.1) [34]. Finally, docking simulations were carried out using Autodock Vina (ver. 1.1.1) [35] in which the exhaustive value was set as 80. The other parameters were left as default values. The three-dimensional box of 40, 40 and 40 Å size, centered at 2.023, 63.29, and 67.062 (*x*, *y*, *z*, respectively) that encompassed the active site of AChE, was used to guide the docked inhibitors within the target enzyme. The lowest energy conformation of each ligand-protein complex was used for analyzing the docking results. The results were depicted using Chimera 1.6 [36].

### Pharmacology

The capacity of target compounds to inhibit AChE/BuChE was assessed using Ellman's method. For this assay, acetylcholinesterase (AChE, E.C. 3.1.1.7, Type V-S, lyophilized powder, from electric eel, 1000 units), butylcholinesterase (BuChE, E.C. 3.1.1.8, from equine serum) and butylthiocholine iodode were purchased from Sigma–Aldrich. 5,5′-Dithiobis-(2-nitrobenzoic acid) (DTNB), potassium, dihydrogen phosphate, dipotassium hydrogen phosphate, potassium hydroxide, sodium hydrogen carbonate, and acetylthiocholine iodide were provided from Fluka. The target compounds were dissolved in 10 mL of a mixture of DMSO/methanol (1:9) and sequentially diluted in phosphate buffer (0.1 M, pH = 8.0) to obtain desired concentrations. For each compound, five different concentrations were selected in such a way to obtain enzymatic inhibition in a range of 20–80%. The rate of absorbance change was measured at 412 nm for 2 min. Aliquots of inhibitors (50 μL) were added to assay solution consisting of phosphate buffer (3 mL, pH = 8, 0.1 M), DTNB (100 μL, 0.01 M), enzyme (50 μL of 2.5 unit/mL) and pre-incubated for 10 min and followed by adding substrate (20 μL, 0.075 M). Assays were carried out with a blank containing all components except enzyme in order to account for the non-enzymatic reaction. All experiments were performed at 25°C in triplicate on a UV Unico double beam spectrophotometer. The reaction rates were compared to obtain the percent of inhibition due to different concentrations of inhibitor. $IC_{50}$ values were determined graphically from log concentration-percent inhibition curves.

### Antioxidant assay

In order to evaluate the total antioxidant power of the target compounds, the FRAP (ferric reducing antioxidant power) assay [37] was used. This method is based on the reduction of colorless Fe(III)-TPTZ (2,4,6-Tris(2-pyridyl)-*s*-triazine) complex to colored Fe(II)-TPTZ complex by the compounds. To 3 mL of FRAP reagent (10 mM TPTZ and 20 mM $FeCl_3$ in 300 mM acetate buffer (pH 3.6)), 100 μL of compounds solution was added and then incubated at 37°C for 15 min. The change of absorbance was measured at 585 nm and the concentration of the reduced Fe(II) was calculated according to the calibration curve of ferrous sulfate ($FeSO_4$) as standard. The antioxidant activity was expressed as mmol Fe(II) per gram of dry mass of compounds. Data are the mean of three independent experiments and are compared to ascorbic acid as reference.

*This work was supported by grants from the research council of Tehran University of Medical Sciences, Iran National Elite Foundation (INEF) and Iran National Science Foundation (INSF). Molecular graphics and analyses were performed with the UCSF Chimera package. Chimera is developed by the 25 Resource for Biocomputing, Visualization, and Informatics at the University of California, San Francisco.*

*The authors have declared no conflict of interest.*

## References

[1] H. Dvir, I. Silman, M. Harel, T. L. Rosenberry, J. L. Sussman, *Chem. Biol. Interact.* **2010**, *187*, 10–22.

 

[2] A. Contestabile, *Behav. Brain Res.* **2011**, *221*, 334–340.

[3] R. C. de Los, *Expert. Opin. Ther. Pat* **2012**, *22*, 853–869.

[4] G. Kryger, I. Silman, J. L. Sussman, *Structure* **1999**, *7*, 297–307.

[5] G. Kryger, I. Silman, J. L. Sussman, *J. Physiol. Paris.* **1998**, *92*, 191–194.

[6] D. Alonso, I. Dorronsoro, L. Rubio, P. Munoz, E. Garcia-Palomero, M. M. Del, A. Bidon-Chanal, M. Orozco, F. J. Luque, A. Castro, M. Medina, A. Martinez, *Bioorg. Med. Chem.* **2005**, *13*, 6588–6597.

[7] P. Camps, X. Formosa, C. Galdeano, D. Munoz-Torrero, L. Ramirez, E. Gomez, N. Isambert, R. Lavilla, A. Badia, M. V. Clos, M. Bartolini, F. Mancini, V. Andrisano, M. P. Arce, M. I. Rodriguez-Franco, O. Huertas, T. Dafni, F. J. Luque, *J. Med. Chem.* **2009**, *52*, 5365–5379.

[8] M. I. Rodriguez-Franco, M. I. Fernandez-Bachiller, C. Perez, B. Hernandez-Ledesma, B. Bartolome, *J. Med. Chem.* **2006**, *49*, 459–462.

[9] W. Luo, Y. P. Li, Y. He, S. L. Huang, D. Li, L. Q. Gu, Z. S. Huang, *Eur. J. Med. Chem.* **2011**, *46*, 2609–2616.

[10] E. Giacobini, R. Spiegel, A. Enz, A. E. Veroff, N. R. Cutler, *J. Neural Transm.* **2002**, *109*, 1053–1065.

[11] E. Giacobini, *Pharmacol. Res.* **2004**, *50*, 433–440.

[12] R. M. Lane, S. G. Potkin, A. Enz, *Int. J. Neuropsychopharmacol.* **2006**, *9*, 101–124.

[13] Y. Furukawa-Hibi, T. Alkam, A. Nitta, A. Matsuyama, H. Mizoguchi, K. Suzuki, S. Moussaoui, Q. S. Yu, N. H. Greig, T. Nagai, K. Yamada, *Behav. Brain Res.* **2011**, *225*, 222–229.

[14] A. Skrzypek, J. Matysiak, A. Niewiadomy, M. Bajda, P. Szymanski, *Eur. J. Med. Chem.* **2013**, *62C*, 311–319.

[15] J. S. da Costa, J. P. Lopes, D. Russowsky, C. L. Petzhold, A. C. Borges, M. A. Ceschi, E. Konrath, C. Batassini, P. S. Lunardi, C. A. Goncalves, *Eur. J. Med. Chem.* **2013**, *62C*, 556–563.

[16] M. Catto, L. Pisani, F. Leonetti, O. Nicolotti, P. Pesce, A. Stefanachi, S. Cellamare, A. Carotti, *Bioorg. Med. Chem.* **2013**, *21*, 146–152.

[17] S. Starcevic, P. Kocbek, G. Hribar, T. L. Rizner, S. Gobec, *Chem. Biol. Interact.* **2011**, *191*, 60–65.

[18] a) H. A. Stefani, K. Gueogjan, F. Manarin, S. H. Farsky, J. Zukerman-Schpector, I. Caracelli, S. R. Pizano Rodrigues, M. N. Muscara, S. A. Teixeira, J. R. Santin, I. D. Machado, S. M. Bolonheis, R. Curi, M. A. Vinolo, *Eur. J. Med. Chem.* **2012**, *58*, 117–127. b) J. Liu, F. Wu, L. Chen, L. Zhao, Z. Zhao, M. Wang, S. Lei, *Food Chem.* **2012**, *135*, 2872–2878. c) R. G. Kalkhambkar, G. M. Kulkarni, C. M. Kamanavalli, N. Premkumar, S. M. Asdaq, C. M. Sun, *Eur. J. Med. Chem.* **2008**, *43*, 2178–2188.

[19] a) M. Khoobi, A. Foroumadi, S. Emami, M. Safavi Gh. Dehghan, B. H. Alizadeh, A. Ramazani, S. K. Ardestani, A. Shafiee, *Chem. Biol. Drug Des.* **2011**, *78*, 580–586. (b) M. Khoobi, S. Emami Gh. Dehghan, A. Foroumadi, A. Ramazani, A. Shafiee, *Arch. Pharm. Chem. Life Sci.* **2011**, *344*, 588–594. (c) M. Khoobi, A. Ramazani, A. Foroumadi, H. Hamadi, Z. Hojjati, A. Shafiee, *J. Iran. Chem. Soc.* **2011**, *8*, 1036–1042.

[20] (a) O. P. Pravin, B. B. Sanjay, D. F. Sandip, K. D. Prashant, T. D. Shailesh, A. P. Dilip, *Bioorg. Med. Chem.* **2013**, *21*, 2434–2450. (b) C. Brühlmann, F. Ooms, P. A. Carrupt, B. Testa, M. Catto, F. Leonetti, C. Altomare, A. Carotti *J. Med. Chem.* **2001**, *44* 19 3195–3198.

[21] H. Nadri, M. Pirali-Hamedani, M. Shekarchi, M. Abdollahi, V. Sheibani, M. Amanlou, A. Shafiee, A. Foroumadi, *Bioorg. Med. Chem.* **2010**, *18*, 6360–6366.

[22] A. V. Terry, Jr., P. M. Callahan, B. Hall, S. J. Webster, *Pharmacol. Biochem. Behav.* **2011**, *99*, 190–210.

[23] L. Pan, J. H. Tan, J. Q. Hou, S. L. Huang, L. Q. Gu, Z. S. Huang, *Bioorg. Med. Chem. Lett.* **2008**, *18*, 3790–3793.

[24] P. Kapkova, V. Alptuzun, P. Frey, E. Erciyas, U. Holzgrabe, *Bioorg. Med. Chem.* **2006**, *14*, 472–478.

[25] R. Palin, J. K. Clark, P. Cowley, A. W. Muir, E. Pow, A. B. Prosser, R. Taylor, M. Q. Zhang, *Bioorg. Med. Chem. Lett.* **2002**, *12*, 2569–2572.

[26] J. K. Clark, P. Cowley, A. W. Muir, R. Palin, E. Pow, A. B. Prosser, R. Taylor, M. Q. Zhang, *Bioorg. Med. Chem. Lett.* **2002**, *12*, 2565–2568.

[27] M. Alipour, M. Khoobi, A. Foroumadi, H. Nadri, A. Moradi, A. Sakhteman, M. Ghandi, A. Shafiee, *Bioorg. Med. Chem.* **2012**, *20*, 7214–7222.

[28] S. Khode, V. Maddi, P. Aragade, M. Palkar, P. K. Ronad, S. Mamledesai, A. H. Thippeswamy, D. Satyanarayana, *Eur. J. Med. Chem.* **2009**, *44*, 1682–1688.

[29] F. Belluti, A. Rampa, L. Piazzi, A. Bisi, S. Gobbi, M. Bartolini, V. Andrisano, A. Cavalli, M. Recanatini, P. Valenti, *J. Med. Chem.* **2005**, *48*, 4444–4456.

[30] H. Pajouhesh, G. R. Lenz, *NeuroRx.* **2005**, *2*, 541–553.

[31] M. A. Lovell, W. R. Markesbery, *J. Neurosci. Res.* **2007**, *85*, 3036–3040.

[32] W. R. Markesbery, M. A. Lovell, *Arch. Neurol.* **2007**, *64*, 954–956.

[33] M. F. Sanner, *J. Mol. Graph. Model.* **1999**, *17*, 57–61.

[34] N. M. O'Boyle, M. Banck, C. A. James, C. Morley, T. Vandermeersch, G. R. Hutchison, *J. Cheminform.* **2011**, *3*, 33.

[35] O. Trott, A. J. Olson, *J. Comput. Chem.* **2010**, *31*, 455–461.

[36] E. F. Pettersen, T. D. Goddard, C. C. Huang, G. S. Couch, D. M. Greenblatt, E. C. Meng, T. E. Ferrin, *J. Comput. Chem.* **2004**, *25*, 1605–1612.

[37] I. F. Benzie, J. J. Strain, *Anal. Biochem.* **1996**, *239*, 70–76.

[38] X. L. Ma, C. Chen, J. Yang, *Acta Pharmacol. Sin.* **2005**, *26*, 500–512.

 